



Highly Independent Triple-band Antenna using Circular Patch Structure for 5G Communication

Yohanes Galih Adhiyoga¹, Tri Nur Arifin², Syaeful Ilman³, Erfiana Wahyuningsih⁴, Dian Rusdiyanto⁵, Adhi Mahendra⁶

^{1,2,3,4}Electrical Engineering Department, Universitas Dian Nusantara

⁵Electrical Engineering Department, Universitas Mercu Buana

⁶Electrical Engineering Department, Universitas Pancasila

^{1,2,3,4}Jakarta Barat, Indonesia 11470

⁵Jakarta Barat, Indonesia 11650

⁶Jakarta Selatan, Indonesia 12630

email: yohanes.galih.adhiyoga@undira.ac.id

ARTICLE INFORMATION

Received 28 July 2023

Revised 13 December 2023

Accepted 26 December 2023

Keywords:

5G communication
circular structure
FDTD simulation
microstrip antenna
multiband antenna

ABSTRACT

5G mobile communication technology has attracted much attention in the past three years. However, the development of antennas that can cover three types of 5G bands at once has not been studied. This paper proposes an antenna covering the three frequency bands of 2.3 GHz, 3.5 GHz, and 26 GHz for 5G communication. The proposed antenna uses a microstrip patch design with 50-ohm inset feeding. Finite Difference Time Domain (FDTD) analysis through simulation has been carried out and confirmed that the proposed antenna meets the required specifications in 5G technology. This is evidenced by the simulation results on the reflection coefficient (S_{11}) parameter, which have values of -22.6 dB, -28.26 dB, and -22.48 dB, respectively. Moreover, from the simulation results, it is known that the proposed antenna possesses gain and efficiency that meet the standards for 5G communication.

1. Introduction

The fifth-generation (5G) cellular technology era is entering the commercialization stage. In this 5G era, use cases that are of particular concern are enhanced mobile broadband (eMBB), ultra-reliable low-latency communications (URLLC), and massive machine-type communications (mMTC) (Huawei, 2016). These three prominent use cases must be supported by high-performance devices so that the benefits of 5G technology can be felt to the fullest. One of the passive components on the device side that is capable of supporting 5G performance is the antenna.

Several frequency bands support the first use case, including ultra-high frequency (UHF), sub-6 GHz, and mmWave (Qualcomm, 2020). Each frequency band is allocated to different applications depending on their coverage or latency requirements. Therefore, an antenna that can cover several frequency bands is needed so that one device has the flexibility to adjust the working frequency band being used.

Although the need for multiband antennas will be needed in the future, recent research has not been done in the literature. As in Przesmycki et al. (2021) and Merlin Teresa & Umamaheswari (2022), the proposed 5G antenna is still only a single band at a frequency of 28 GHz. In the following year, there have been several researchers who proposed dual-band 5G antennas, such as Sun et al. (2021) which succeeded in realizing the 23 GHz and 42 GHz frequencies, and Guo et al. (2021) in the microwave band (4.85 GHz) and millimeter-wave (26 GHz). In addition, recent research on 5G multiband antennas has been proposed by Al-Khaylani et al. (2022), proving the antenna works at 3.6 GHz, 3.9 GHz, and 4.9 GHz frequencies. However, even though it already has a variety of working frequencies, the working spectrum used is still in the S-band and C-band. Therefore, this study proposes a microstrip antenna design with triple-band characteristics at a 5G frequency.

Each of these frequencies can be set independently by modifying the dimensions of each structure related to its operating frequency. Each working frequency produced has good performance in several standard antenna parameters.

In this study, prior to commencing the antenna design process, various references were gathered, and relevant literature on antenna design, antenna specifications, and the characteristics of each antenna parameter were studied. Following this, the antenna design, simulation, and optimization processes were initiated. The workflow of this research can be observed in Figure 1.

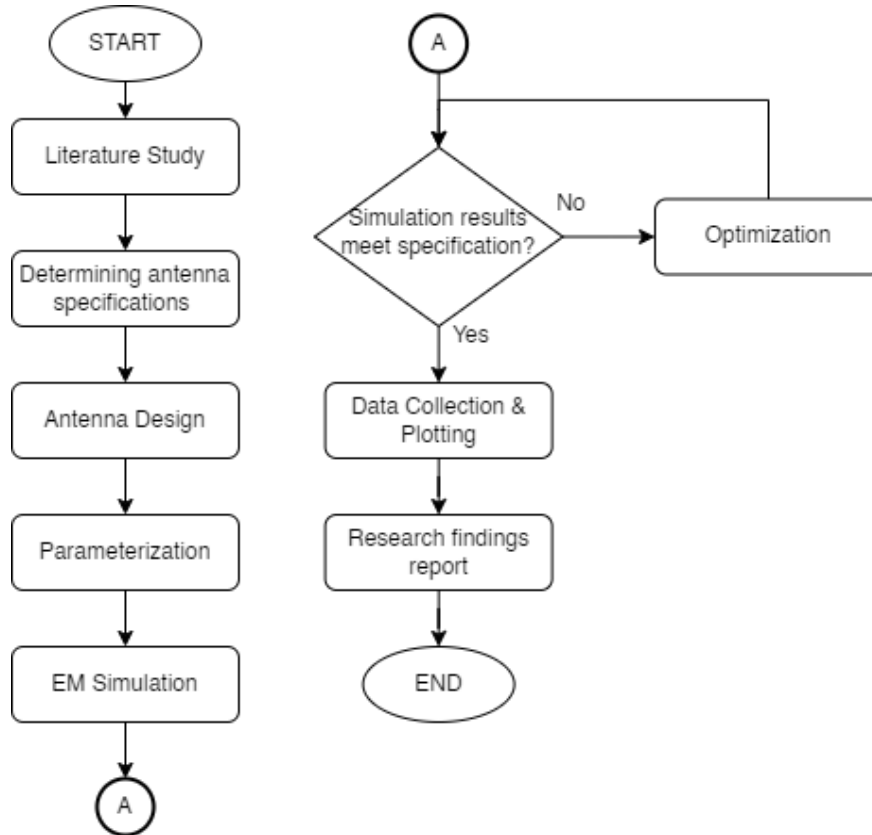


Figure 1. Research Workflow

2. Antenna Design

The microstrip antenna characteristics are not only determined by its material but also by the shape of the resonator. The shape of these resonators could be determined by the amount of resonance produced by the antenna (Boursianis et al., 2020). The more resonances produced, the more complex the shape of the resonator will be. Several studies have shown that multiband characteristics can be produced by modifying the shape of the antenna resonator (Abdalla & Hu, 2018; Hussain et al., 2020) or by providing two feeders simultaneously in one patch antenna design (Amelia et al., 2018). Hussain et al. (2020) produce multiband characteristics by adding a U-shaped slot structure at 28 GHz and 38 GHz frequencies. In line with that, Abdalla and Hu (2018) also utilize a modified resonator using an additional three meander line structures to produce quadband characteristics at sub-6 GHz. In line with the result mentioned earlier, in this study, the microstrip antenna is designed to have resonance at three 5G working frequencies, namely in the UHF, sub-6 GHz, and mmWave bands, by modifying the resonator. These resonant frequencies can be controlled by their respective dimensions in each structure. by modifying the resonator.

2.1. Circular Patch Design

The proposed antenna structure uses a basic ring shape as an initial frequency generator with a diameter parameter to adjust the frequency. Several considerations were taken into account in designing the main ring shape, including the outer ring radius, the inner ring radius, and the gap from the ring to the patch (Kisel et al., 2016). Meanwhile, a circular structure is placed in the ring with additional slits and insets for other frequencies. In addition to serving as a creator of multiband characteristics, this structure is also utilized for antenna impedance matching. The proposed antenna design with the shape of a ring, circular patch, slit, and inset resonator is shown in Figure 2.

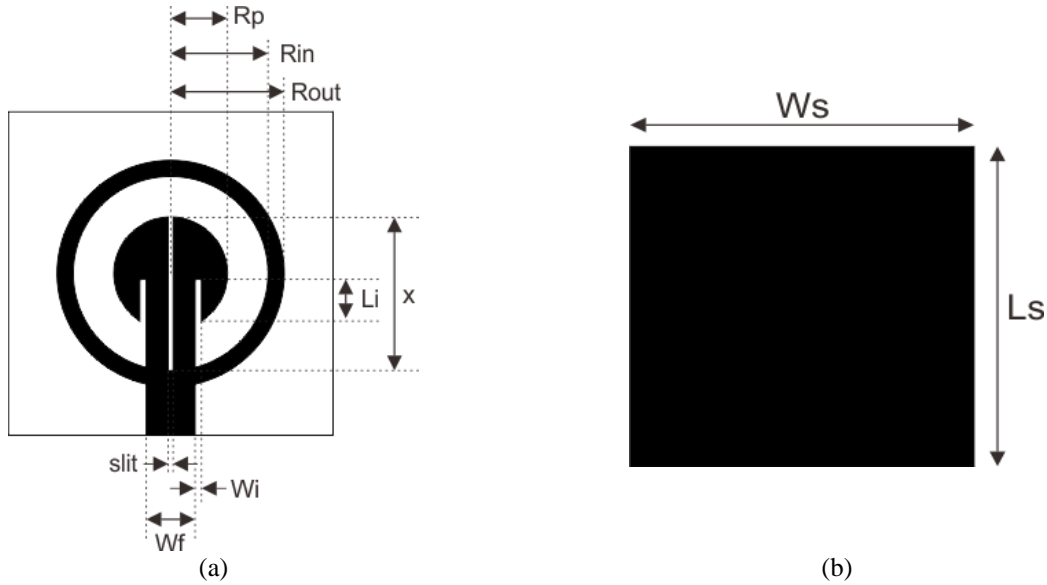


Figure 2. Design of the proposed antenna: (a) Patch side; (b) Ground plane side

The dimensions of the circular patch designed in this study were obtained based on the calculations using the basic formula for the resonance frequency at (Balanis, 2016), which was then optimized to obtain the dimensions of each parameter, as shown in Table 1.

Table 1. Optimized antenna dimensions

No	Symbol	Value (mm)	Description
1	L_s	20	Substrate length
2	W_s	20	Substrate width
3	R_{in}	6	Inner ring radius
4	R_{out}	7	Outer ring radius
5	R_p	3.5	Patch radius
6	h	1.6	Substrate thickness
7	t	0.035	Patch thickness
8	W_f	10	Feed width
9	L_i	2.8	Inset length
10	W_i	0.4	Inset width
11	x	10	Slit length
12	$slit$	0.3	Slit width

In this study, an FR-4 dielectric material with a thickness of 1.6 mm was used with a relative permittivity of 4.6. At the front of the antenna is a patch structure, and the back is equipped with a ground plane covering the entire substrate. This antenna is fed directly via a microstrip line, adding a 50Ω inset feeding structure.

2.2. Controllable Frequency

The flexibility of an antenna could be measured by how easily the antenna design is adjusted to achieve a specific working frequency. In general, the frequency can be adjusted by the dimensions of the antenna resonator; the larger the resonator, the lower the working frequency, and vice versa (Hansen, 1981). Referring to this principle, the antenna design proposed in this study can independently allocate each patch structure block at its frequency. Due to the use of three frequencies at once, the changes in one structure in each band were designed not to affect each other's working frequencies in other bands. Indeed, one block of the resonator structure only affects the working frequency in one band.

This tuning process can be done in various ways, such as using active components (Asif et al., 2019; Bai et al., 2017), using split-ring resonators (SRR) (Zaidi et al., 2020), or adding decoupling elements (Xu et al., 2017). Qiang (Bai et al., 2017) has succeeded in designing a tri-band tunable antenna that utilizes a varactor diode and a tunable capacitor as components to minimize mutual coupling between radiating elements when the frequency is varied. The same thing was also done by Sajid (Asif et al., 2019), who realized a quad-band antenna in the sub-6 GHz frequency range. Another technique is done by Zaidi (Zaidi et al., 2020), who has successfully designed a tri-band antenna in the sub-6 GHz range. These three frequency bands can be set independently without affecting the performance of antennas on other spectrums. The structure of the hexagonal split-ring resonator is used to make it able to tune the resonant at the desired frequency.

In this research, the principle is almost the same as Zaidi's, namely by utilizing the resonator structure to adjust the frequency in each band. When viewed from the shape of the patch, the antenna proposed in this study has a central arrangement in the form of a ring structure, representing the lowest frequency. The other two resonances are formed from additional structures in the ring, solid circles separated by a slit structure that seems to separate from one another. These two parts make other resonances at higher frequencies, namely in the sub-6 GHz and mmWave frequencies. In the end, the three parts of the patch structure were fed simultaneously by microstrip line feeding, which is optimized with an inset structure as an antenna matching impedance.

3. Results and Discussions

The proposed antenna design is then analyzed through simulation to determine its performance if the antenna is realized. The simulation is run using CST Microwave Studio software by considering several conditions close to actual conditions in the field. The antenna parameters that are simulated in this study include S-Parameter, Efficiency, Gain, and Radiation Pattern.

The working frequency of the antenna formed from the proposed microstrip antenna design was verified through the analysis of the S-Parameter. One of the parameters reviewed is the reflection coefficient (S_{11}). The simulation results of the proposed antenna for parameter S_{11} were shown in Figure 3.

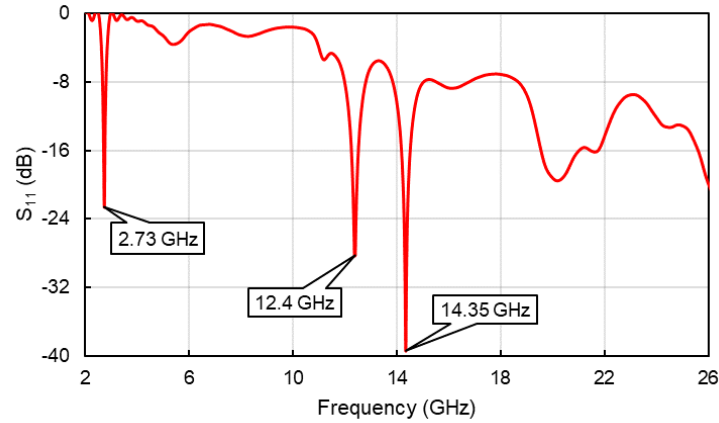


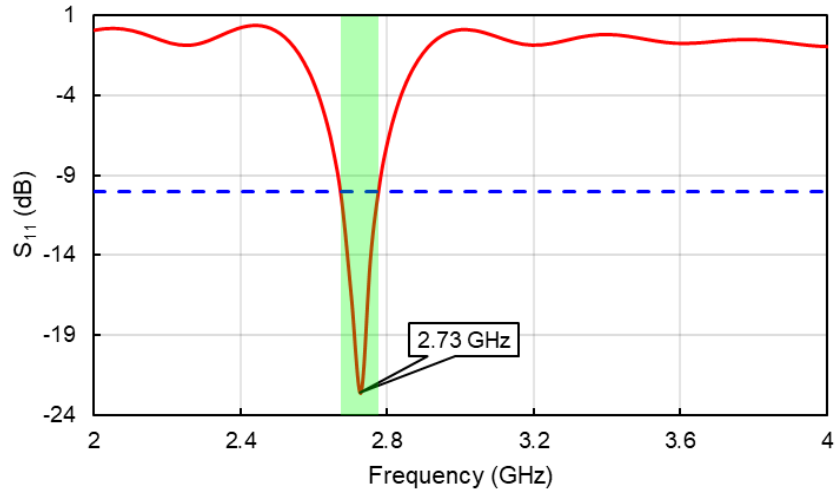
Figure 3. Simulation results of S_{11} parameters at three resonant frequencies

Based on Figure 3, it can be seen that the proposed antenna has three resonances, namely at frequencies of 2.7 GHz, 12.4 GHz, and 14.3 GHz. The three obtained frequencies indicate that this proposed antenna is highly adaptable to adjust its frequency to the three 5G frequency bands, as mentioned earlier. This possibility is supported by the independence of the antenna structure, where each part is associated with only one frequency band. Therefore, changing the dimensions of one part will not interfere with the frequencies that have already been successfully formed.

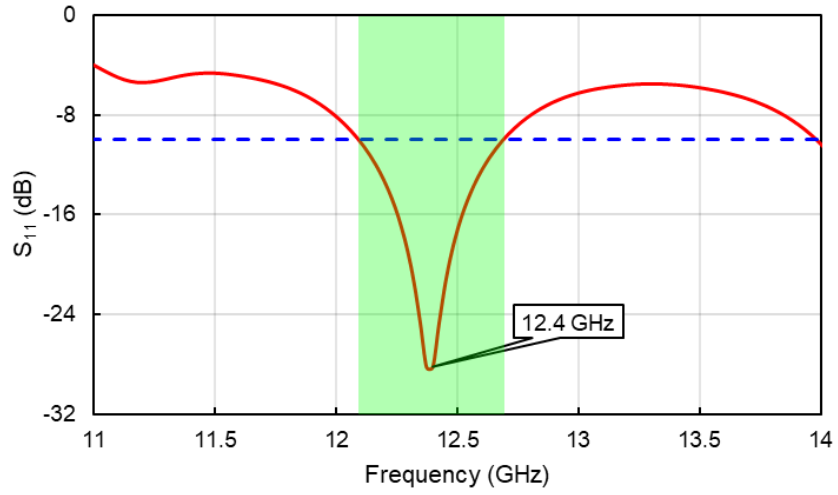
Based on the simulation results, these these frequencies has a reasonably good reflection coefficient value of less than -20 dB, where this value proves that the antenna has an impedance that matches the target of 50Ω . If viewed in more detail, then at the first resonance, by taking the reflection coefficient limit of -10 dB, this antenna has a bandwidth of 100 MHz (Figure 4a), which is sufficient for the needs of 5G technology. The green-colored area illustrates the antenna bandwidth generated at the specified operating frequency.

At the second and third resonances, which can be seen in Figures 4b and 4c, it is known that the resulting bandwidth is much larger than the first resonance. This is because when the frequency is higher, the resulting bandwidth, gain, and efficiency will also be more significant (Adhiyoga et al., 2019). At the second resonance at a frequency of 12.4 GHz, the resulting bandwidth is 600 MHz, while at the third resonance at a frequency of 14.35 GHz, a bandwidth of 770 MHz is obtained.

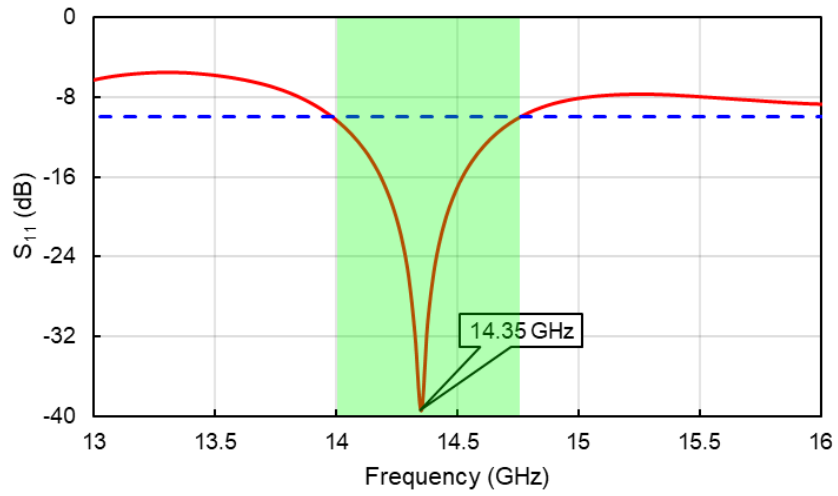
Based on these results, it can be proven that the designed microstrip antenna is capable of producing three resonances that work at different frequencies. These three resonances also have impedances that match adequate bandwidth to be applied to 5G technology both on the uplink and downlink sides.



(a)



(b)



(c)

Figure 4. Antenna bandwidth at each resonance: (a) 2.7 GHz, (b) 12.4 GHz, and (c) 14.3 GHz

Another parameter that is reviewed in this study is efficiency. In general, the efficiency of microstrip antennas is influenced by the ratio between the resonator's area and the antenna's dimensions. The wider the resonator field compared to the antenna dimensions, the higher the efficiency. As conveyed by (Yang et al., 2021), the inclusion of additional structures in patch structures may represent conductor properties, resulting in a potential reduction in antenna efficiency. However, because the proposed antenna's patch design (resonator) has many indentations and slots to produce multiband characteristics, the antenna's efficiency cannot be maximized.

The simulation results for this efficiency parameter can be seen in Figure 5. In the figure, markers represent each resonant frequency at 2.728 GHz, 12.4 GHz, and 14.35 GHz. These three successfully obtained frequencies can be independently configured to operate within the targeted range by conducting a parametric study on antenna dimensions, specifically on parameters such as the ring radius (R_{in} and R_{out}), circular patch radius (R_p), and slit width (*slit*) as a frequency divider.

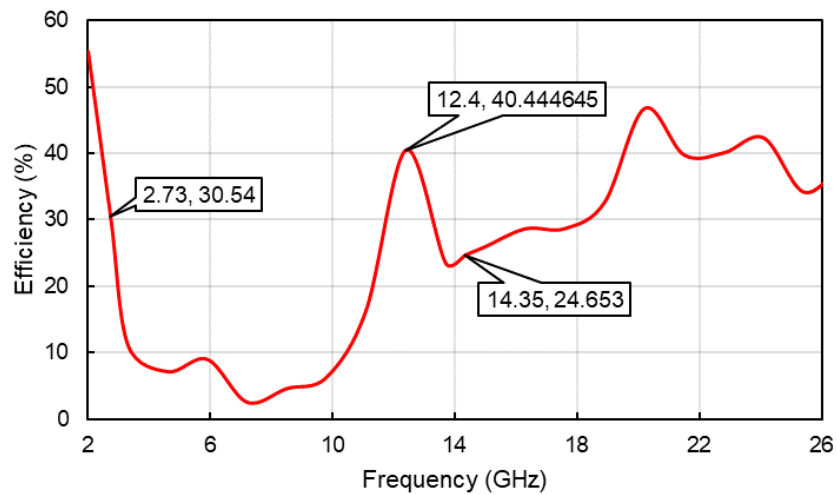


Figure 5. Antenna efficiency simulation results at three resonant frequencies

Based on the simulation results in Figure 5, it is known that the highest efficiency is achieved at the second resonance, which is 40.4%, followed by the first resonance at 30.5% and the third at 24.65%. This condition indicates that there are still quite significant losses causing low efficiency. These losses occur due to many gaps in the patch design, which causes the current distribution to be not smooth, from which it should be transmitted directly but becomes blocked by the gaps formed. Based on the trend, this efficiency is proportional to the antenna impedance value, where the better the impedance, the better the efficiency.

With the efficiency value as stated above, it can also be seen that the antenna gain will show the same trend. However, based on the simulation results for the gain parameter shown in Figure 6, the proposed antenna can still provide a positive gain response at the second resonant frequency.

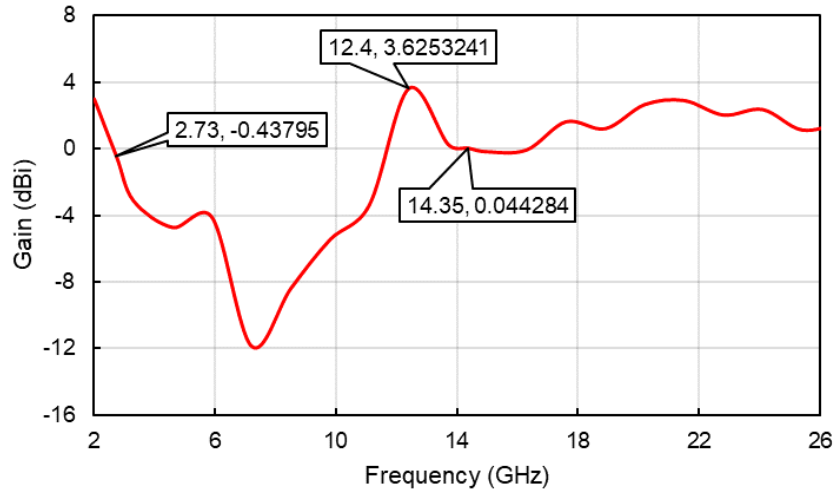


Figure 6. Antenna gain simulation results at three resonant frequencies

Figure 6 shows that at the first resonance, the gain is -0.438 dBi, while at the second resonance, it is 3.624 dBi, and at the third resonance, it is 0.044 dBi. These results show that, as in the previous efficiency, the gain is also directly proportional to the antenna impedance, which has the best value at the second resonance. This parameter is also very dependent on the antenna substrate used and the substrate’s thickness, so a higher gain can be obtained if a substrate with a lower permittivity and dielectric loss is used. In this study, a substrate of dielectric material FR-4 was used with a relative permittivity (ϵ_r) of 4.6 and a dielectric loss ($\tan \delta_e$) of 0.025. With the reasonably large dispersive properties of the material, it will also affect the increasing losses so that antenna gain can be sacrificed.

The last parameter reviewed in this study is the antenna radiation pattern. This parameter can describe the beam’s direction and the signal reception level that the receiver will receive. In general, the proposed antenna has a directional radiation pattern on the positive z -axis of the antenna with a realized gain of 2.3 dBi, as shown in Figure 7.

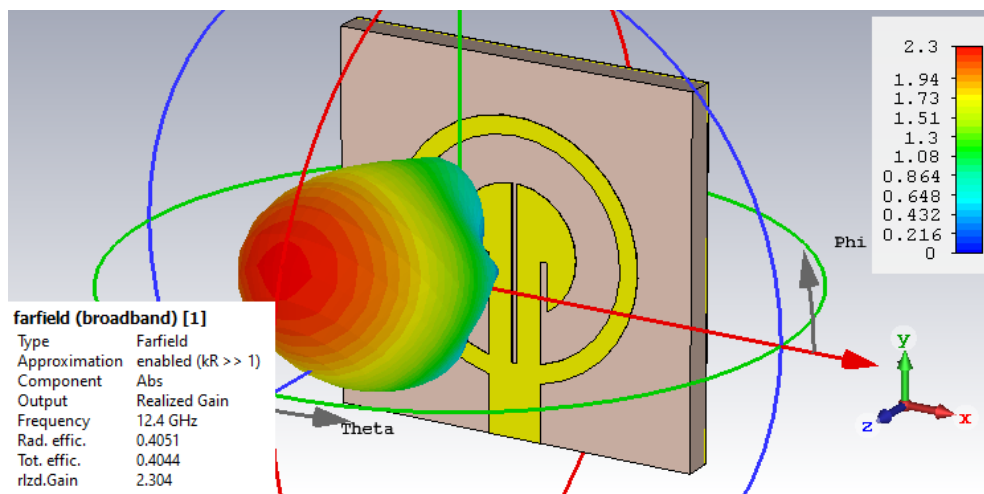


Figure 7. The radiation pattern of the simulated antenna at a frequency of 12.4 GHz

The radiation pattern result follows its designation, which does not require a beam behind the antenna (bidirectional). This is also one of the microstrip antenna characteristics which does not produce a radiation

pattern behind the antenna. The role of the antenna ground plane is what causes the electromagnetic wave emission to be wholly distributed toward the front of the antenna. A polar diagram is also used for more detail in analyzing the antenna's radiation pattern, as shown in Figure 8.

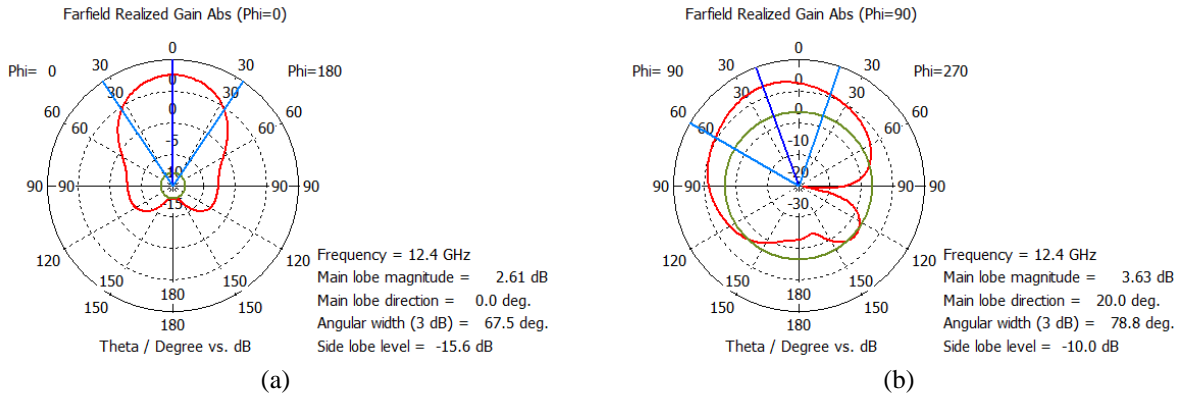


Figure 8. Simulation results of the antenna radiation pattern in the polar diagram at a frequency of 12.4 GHz: (a) $\phi = 0^\circ$; (b) $\phi = 90^\circ$

Figure 8 more clearly describes the beam's direction from the antenna designed at a frequency of 12.4 GHz. The emission pattern at $\phi = 0^\circ$ is known to have a Half Power Beam Width (HPBW) of 67.5° (Figure 8a). While at $\phi = 90^\circ$, the resulting HPBW is 78.8° (Figure 8b). This result is very suitable if the antenna is used as a cellular antenna that requires a large enough HPBW to cover a specific area. In addition, based on the simulation results, it can be seen that the emitted beam has a tilt angle of 20° to the y-axis, so if it is to be implemented to obtain a direction that has a maximum gain, the reference of 20° from the normal axis can be used.

Based on numerical analysis using the FDTD method, the proposed antenna, apart from having various resonance frequencies in the three 5G bands, also has convenience in the tuning process, which is independent. Each part of the patch has an independent effect on the frequency shift, which facilitates the frequency-matching process. In terms of gain and radiation pattern, it can be seen that although not all frequency bands have high gain, this antenna can still easily arrange in an array so that the gain can be increased. Another exciting thing from the results was the radiation pattern, where the same characteristics were obtained from the simulation results in the three frequency bands, each of which has a relatively large beamwidth on the $\phi = 0^\circ$ axes. In addition, on the $\phi = 90^\circ$ axes, the proposed antenna has a beam directed to the second quadrant, which will facilitate the tilting process when the antenna is implemented as a cellular antenna.

4. Conclusion

Based on the research data, it can be concluded that the multiband microstrip antenna has been successfully designed, simulated, and reviewed for its performance. The antenna can work simultaneously in three resonant frequency ranges: the UHF frequency of 2.728 GHz, millimeter wave at 12.4 GHz, and 14.35 GHz. Each resonance has a frequency set by modifying the dimensions of its respective structure without affecting the characteristics of S_{11} at other frequencies. In addition, the three operating frequencies of the antenna have sufficient bandwidth to be applied to 5G technology, with the enormous bandwidth being in the third resonance. The antenna gain has met the minimum criteria because the gain is positive up to 3.6 dBi at the second resonance. Meanwhile, the antenna radiation pattern has a directional beam characteristic with a beamwidth of 78.8° , which radiates towards 20° from the normal axis.

Some of the results of this analysis are broadly sufficient to meet the criteria for applying 5G technology which will occupy three different frequency bands. This antenna is designed to answer the challenge where one antenna not only can work on one frequency but three at once, each of which has good performance.

5. Acknowledgements

This work was supported in part by the Directorate General of Higher Education, Research, and Technology in terms of Penelitian Dosen Pemula (PDP) under Grant No: 1406/LL3/AL.04/2023. The author also would like to thank Institute for Research and Community Service Universitas Dian Nusantara for the research facility support.

References

- Abdalla, M. A., & Hu, Z. (2018). Design and analysis of a compact quad band loaded monopole antenna with independent resonators. *International Journal of Microwave and Wireless Technologies*, 10(4), 479–486.
- Adhiyoga, Y. G., Apriono, C., & Rahardjo, E. T. (2019). Bandwidth and Gain Improvement using Artificial Magneto-dielectric Material with Split-Ring Resonator Array Configuration. *2019 IEEE Conference on Antenna Measurements & Applications (CAMA)*, 261–264. <https://doi.org/10.1109/CAMA47423.2019.8959545>
- Al-Khaylani, H. H., Elwi, T. A., & Ibrahim, A. A. (2022). A novel miniaturized reconfigurable microstrip antenna based printed metamaterial circuitries for 5G applications. *Prog. Electromagn. Res*, 120, 1–10.
- Amelia, F., Adhiyoga, Y. G., Zulkifli, F. Y., & Rahardjo, E. T. (2018). Microstrip Antenna Design with Dual Linear Polarizations for X-Band Weather Radar Applications. *2018 International Conference on Radar, Antenna, Microwave, Electronics, and Telecommunications (ICRAMET)*, 90–93. <https://doi.org/10.1109/ICRAMET.2018.8683910>
- Asif, S. M., Anbiyaei, M. R., Ford, K. L., O'Farrell, T., & Langley, R. J. (2019). Low-profile independently-and concurrently-tunable quad-band antenna for single chain sub-6GHz 5G new radio applications. *IEEE Access*, 7, 183770–183782.
- Bai, Q., Singh, R., Ford, K. L., O'Farrell, T., & Langley, R. J. (2017). An independently tunable tri-band antenna design for concurrent multiband single chain radio receivers. *IEEE Transactions on Antennas and Propagation*, 65(12), 6290–6297.
- Balanis, C. A. (2016). *Antenna theory: analysis and design*. John wiley & sons.
- Boursianis, A. D., Papadopoulou, M. S., Pierezan, J., Mariani, V. C., Coelho, L. S., Sarigiannidis, P., Koulouridis, S., & Goudos, S. K. (2020). Multiband patch antenna design using nature-inspired optimization method. *IEEE Open Journal of Antennas and Propagation*, 2, 151–162.
- Guo, Y. Q., Pan, Y. M., Zheng, S. Y., & Lu, K. (2021). A Singly-Fed Dual-Band Microstrip Antenna for Microwave and Millimeter-Wave Applications in 5G Wireless Communication. *IEEE Transactions on Vehicular Technology*, 70(6), 5419–5430. <https://doi.org/10.1109/TVT.2021.3070807>
- Hansen, R. C. (1981). Fundamental limitations in antennas. *Proceedings of the IEEE*, 69(2), 170–182.
- Huawei. (2016). *5G Spectrum - Public Policy Position*. Public Policy Position. https://www-file.huawei.com/-/media/CORPORATE/PDF/public-policy/public_policy_position_5g_spectrum.pdf
- Hussain, W., Khattak, M. I., Khattak, M. A., & Anab, M. (2020). Multiband microstrip patch antenna for 5G wireless communication. *International Journal, Of, Engineering, Works*, 7(1), 15–21.
- Kisel, N. N., Cheremisov, V. A., & Derachitc, D. S. (2016). The modeling of characteristics of the patch antenna with non-uniform substrate metamaterial. *2016 IEEE East-West Design & Test Symposium (EWDTS)*, 1–3.
- Merlin Teresa, P., & Umamaheswari, G. (2022). Compact Slotted Microstrip Antenna for 5G Applications Operating at 28 GHz. *IETE Journal of Research*, 68(5), 3778–3785. <https://doi.org/10.1080/03772063.2020.1779620>
- Przesmycki, R., Bugaj, M., & Nowosielski, L. (2021). Broadband Microstrip Antenna for 5G Wireless Systems Operating at 28 GHz. In *Electronics* (Vol. 10, Issue 1). <https://doi.org/10.3390/electronics10010001>
- Qualcomm. (2020). *Global update on spectrum for 4G & 5G*. Qualcomm Inc., San Diego, CA, White Paper. <https://www.qualcomm.com/media/documents/files/spectrum-for-4g-and-5g.pdf>
- Sun, W., Li, Y., Chang, L., Li, H., Qin, X., & Wang, H. (2021). Dual-Band Dual-Polarized Microstrip Antenna Array Using Double-Layer Gridded Patches for 5G Millimeter-Wave Applications. *IEEE Transactions on Antennas and Propagation*, 69(10), 6489–6499. <https://doi.org/10.1109/TAP.2021.3070185>
- Xu, H., Zhou, H., Gao, S., Wang, H., & Cheng, Y. (2017). Multimode decoupling technique with independent tuning characteristic for mobile terminals. *IEEE Transactions on Antennas and Propagation*, 65(12), 6739–6751.
- Yang, S. J., Yang, Y., & Zhang, X. Y. (2021). Low scattering element-based aperture-shared array for multiband base stations. *IEEE Transactions on Antennas and Propagation*, 69(12), 8315–8324.
- Zaidi, A., Awan, W. A., Hussain, N., & Baghdad, A. (2020). A Wide and Tri-band Flexible Antennas with Independently Controllable Notch Bands for Sub-6-GHz Communication System. *Radioengineering*, 29(1).